Extraction of Density of States in Amorphous GaInZnO Thin-Film Transistors by Combining an Optical Charge Pumping and Capacitance–Voltage Characteristics

Jun-Hyun Park, Kichan Jeon, Sangwon Lee, Sunil Kim, Sangwook Kim, Ihun Song, Chang Jung Kim, Jaechul Park, Youngsoo Park, Dong Myong Kim, *Member, IEEE*, and Dae Hwan Kim, *Member, IEEE*

***Abstract*—A technique for extracting the acceptorlike density of states (DOS) of n-channel amorphous GaInZnO (a-GIZO) thin-film transistors based on the combination of subbandgap optical charge pumping and C–V characteristics is proposed. While the energy level is scanned by the photon energy and the gate voltage sweep, its density is extracted from the optical response of C–V characteristics. The extracted DOS shows the superposition of the exponential tail states and the Gaussian deep states ($N_{\mathrm{TA}} = 2 \times 10^{18}\ \mathrm{eV}^{-1} \cdot \mathrm{cm}^{-3}$, $N_{\mathrm{DA}} = 4 \times 10^{15}\ \mathrm{eV}^{-1} \cdot \mathrm{cm}^{-3}$, $kT_{\mathrm{TA}} = 0.085$ eV, $kT_{\mathrm{DA}} = 0.5$ eV, $E_O = 1$ eV). The TCAD simulation results incorporated by the extracted DOS show good agreements with the measured transfer and output characteristics of a-GIZO thin-film transistors with a single set of process-controlled parameters.**

***Index Terms*—Amorphous, density of states (DOS), GaInZnO (GIZO), optical response, TCAD, thin-film transistors.**

I. Introduction

MULTICOMPONENT amorphous oxide semiconductor-based thin-film transistors (TFTs) (i.e., GaInZnO (GIZO), InZnO, and GaZnO) have been under active research and development because of their room temperature (RT) fabrication process, low cost, higher mobility than those of covalent semiconductor TFTs, and compatibility with transparent and rollable electronics applications. Because the electrical characteristics of GIZO TFTs are mainly dependent on both the electron concentration (n) and the density of states (DOS: $g(E)$) of the GIZO active layer, the extraction of n and $g(E)$ is very important in the modeling and characterization of their devices and circuits. While n is known to be determined by process conditions, i.e., oxygen vacancies [1], [2] and radio frequency (RF) power in sputtering [3], and has experimentally been extracted by many groups [2]–[5] (from, e.g., Hall measurement or electrical characteristics), the extraction of $g(E)$ has rarely been investigated or recently studied only by the numerical simulation-based fitting [6], [7].

Manuscript received August 8, 2008; revised September 6, 2008. This work was supported by the research project of Samsung Advanced Institute of Technology, and the CAD softwares were supported by SILVACO and IC Design Education Center (IDEC). The review of this letter was arranged by Editor J. K. O. Sin.

J.-H. Park, K. Jeon, S. Lee, D. M. Kim, and D. H. Kim are with the School of Electrical Engineering, Kookmin University, Seoul 136-702, Korea (e-mail: jhpark@kookmin.ac.kr; kchjeon@kookmin.ac.kr; no1.sangwon@gmail.com; dmkim@kookmin.ac.kr; drlife@kookmin.ac.kr).

S. Kim, S. Kim, I. Song, C. J. Kim, J. Park, and Y. Park are with the Semiconductor Laboratory, Samsung Advanced Institute of Technology, Giheung-Gu, Yongin-Si, Gyeonggi-Do 446-712, Korea (e-mail: sunnil.kim@samsung.com; nofate.kim@samsung.com; ihsong@samsung.com; cj2.kim@samsung.com; jackpot.park@samsung.com; uvip@samsung.com).

Digital Object Identifier 10.1109/LED.2008.2006415

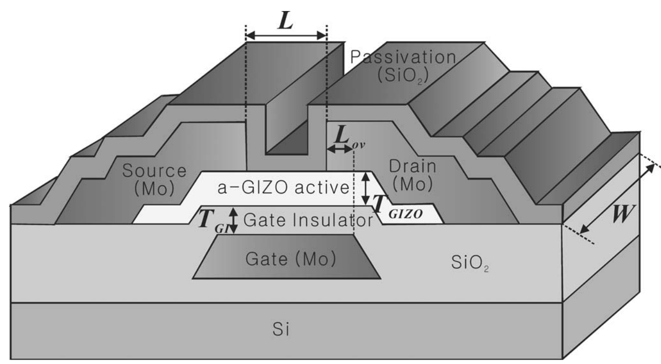

Fig. 1. Schematic diagram of the fabricated a-GIZO TFT which has an inverted staggered bottom gate structure.

In this letter, the extraction method of $g(E)$ of n-channel GIZO TFTs (acceptorlike DOS) by combining subbandgap optical charge pumping and capacitance–voltage (C–V) characteristics is proposed. In addition, TCAD simulation results incorporated by extracted acceptorlike DOS are compared with the measured characteristics.

II. Device Fabrication

A schematic cross section of integrated GIZO TFTs with the most commonly used staggered bottom gate structure for active-matrix liquid crystal displays is shown in Fig. 1. On a thermally grown SiO_2/Si substrate, the first sputtered deposition at RT and patterning of a molybdenum (Mo) gate are followed by PECVD deposition of a 100-nm-thick SiO_2 at 300 °C (gate insulator thickness $T_{\mathrm{GI}} = 100$ nm). A 70-nm-thick active layer ($Ga_2O_3 : In_2O_3 : ZnO$ = 2:2:1 at %) is then sputtered by the RF magnetron sputtering at RT in a mixed atmosphere of Ar/O_2 (100:1 at sccm) and wet-etched with

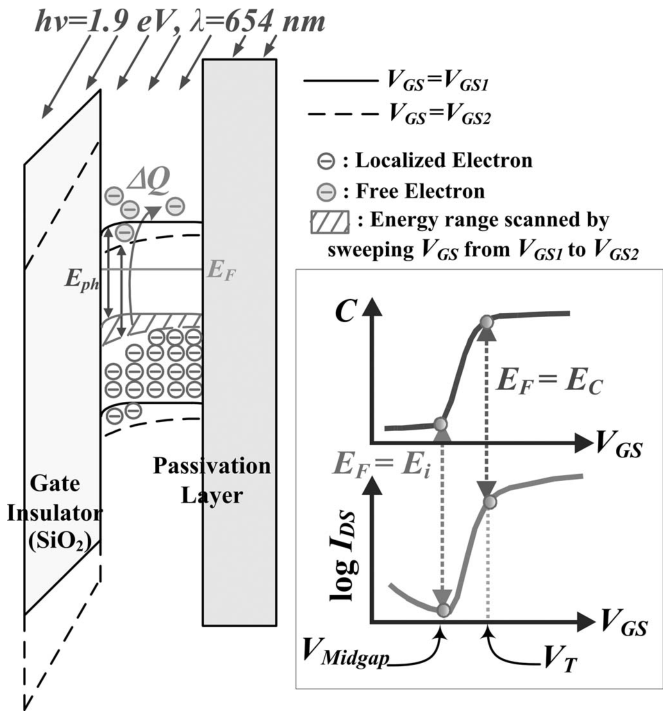

Fig. 2. Illustrative concept of the extraction of a-GIZO DOS [$g(E)$] based on an optical charge pumping technique. The difference of C_{GIZO} between V_{GS1} and V_{GS2} is converted into the $g(E)$ in the range of $(E_F - E_i)$ modulated by $V_{\mathrm{GS1}} \sim V_{\mathrm{GS2}}$. The range of energy level can be controlled by both E_{ph} and V_{GS}. The inset shows the relationship between V_{GS} and the energy level in $g(E)$.

diluted HF (GIZO active layer thickness $T_{\mathrm{GIZO}} = 70$ nm). For the source/drain (S/D) pattern, a 200-nm-thick layer of Mo is sputtered at RT and then patterned by dry etching. After N_2O plasma treatment on the channel surface of the GIZO active layer, a SiO_2 passivation layer is continuously deposited at 150 °C by PECVD without a vacuum break. Finally, all the samples were annealed for 1 h in the furnace at 250 °C. The channel length (L), the channel width (W), and the length of the overlap region between the gate and S/D (L_{ov}) are designed to be 50, 200, and 10 μm, respectively. It was confirmed that the fabricated GIZO layer has an amorphous phase (a-GIZO) by XRD view (not shown here) and showed the *n-type* amorphous oxide semiconductor property [1].

III. Experimental Results and Discussion

In order to extract the distribution of DOS $g(E)$, the optical capacitance–voltage (C–V) response between the gate and S/D electrodes in the a-GIZO TFT is employed utilizing the difference of measured capacitance between the dark (C_{dark}) and photon-illuminated states (C_{photo}) as a function of the gate voltage (V_{GS}). Fig. 2 shows the concept of the proposed optical charge pumping technique. The optical source is guided to the Cascade Microtech's Optical Probe Head through a multimode fiber with a diameter $= 50$ μm. Optical fiber is placed over the a-GIZO active layer of the device under characterization. An optical source with a subbandgap photon energy ($\lambda = 654$ nm, $E_{\mathrm{ph}} = 1.90$ eV $< E_{g,\mathrm{GIZO}} \approx 3.2$ eV, and maximum optical power $P_{\mathrm{opt}} = 50$ mW) is employed to pump trapped electrons

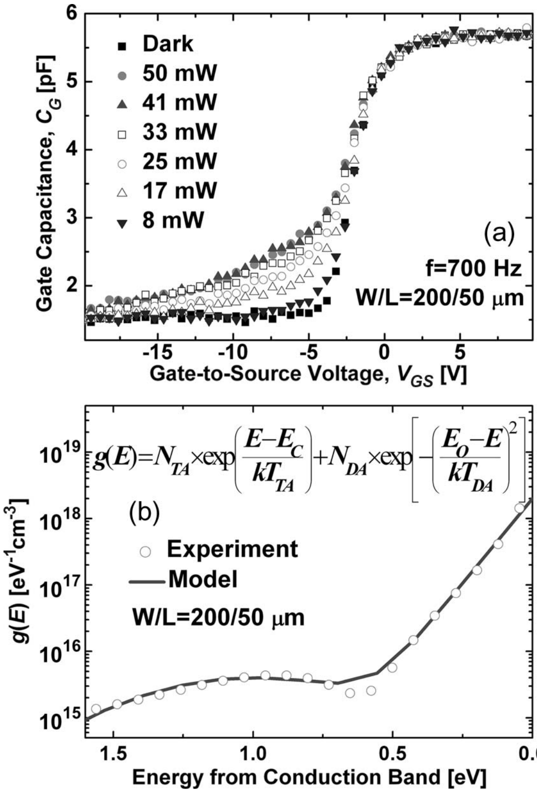

Fig. 3. (a) Optical power (P_{opt}) dependence of C–V measurement in a-GIZO TFT. The $g(E)$ extraction was performed at $P_{\mathrm{opt}} = 50$ mW. (b) Consequently extracted $g(E)$ and its characteristic equation. (Symbol: $g(E)$ as extracted by the proposed method. Line: $g(E)$ incorporated into TCAD model).

in localized states $g(E)$ from the energy level below the Fermi level E_F to the a-GIZO conduction band minimum E_C by the specific E_{ph} while excluding the band-to-band electron-hole pair generation in the a-GIZO layer.

By modeling C_{dark} and C_{photo} as

$$\frac{1}{C_{\mathrm{dark}}(V_{\mathrm{GS}})} = \frac{1}{C_{\mathrm{ox}}} + \frac{1}{C_B(V_{\mathrm{GS}})} \ [\mathrm{F}^{-1}] \quad (1)$$

$$\frac{1}{C_{\mathrm{photo}}(V_{\mathrm{GS}})} = \frac{1}{C_{\mathrm{ox}}} + \frac{1}{C_B(V_{\mathrm{GS}}) + C_{\mathrm{GIZO}}(V_{\mathrm{GS}})} \ [\mathrm{F}^{-1}] \quad (2)$$

C_{GIZO} can be extracted as a function of V_{GS} from

$$\begin{aligned} C_{\mathrm{GIZO}}(V_{\mathrm{GS}}) &= \frac{\Delta Q}{\Delta V_{\mathrm{gs}}} \\ &= \frac{q\Delta N}{\Delta V_{\mathrm{gs}}} \\ &= C_{\mathrm{ox}} \left[\frac{C_{\mathrm{photo}}}{C_{\mathrm{ox}} - C_{\mathrm{photo}}} - \frac{C_{\mathrm{dark}}}{C_{\mathrm{ox}} - C_{\mathrm{dark}}} \right] \ [\mathrm{F}] \end{aligned} \quad (3)$$

with C_{ox} as the gate oxide insulator capacitance, C_B as the capacitance due to V_{GS}-responsive localized trapped charge in a-GIZO active layer under dark state, C_{GIZO} as the capacitance due to photoresponsive charges (ΔQ) and/or electrons (ΔN)

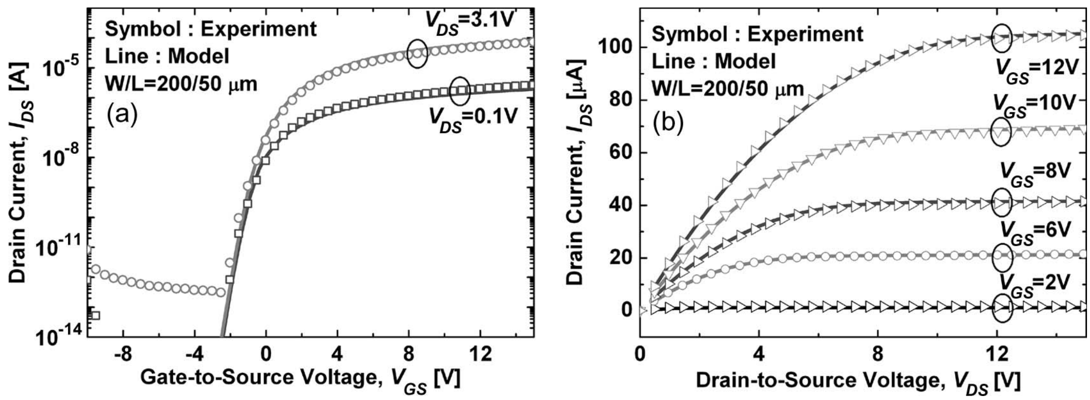

Fig. 4. (a) Measured transfer characteristics and (b) output characteristics of a-GIZO TFT. The model based on extracted $g(E)$ agrees very well with measured characteristics over the wide range of $V_{\rm GS}$ and $V_{\rm DS}$ (with the fixed process-controlled parameters).

at a fixed $V_{\rm GS}$, and $\Delta V_{\rm gs}$ as the small signal voltage in C–V measurement. Since $C_{\rm ox}$ can be calculated, $C_{\rm GIZO}$ can be also extracted from (3). As a result of the conversion of ΔN to the photoresponsive electron density $\Delta n[\rm cm^{-3}]$ with

$$\Delta N(V_{\rm GS}) = \pi r^2 \times T_{\rm GIZO} \int_{E_C(V_{\rm GS})-E_{\rm ph}}^{E_F} g(E)dE \qquad (4)$$

$$\begin{aligned}\Delta C'_{\rm GIZO} &= \frac{C_{\rm GIZO}(V_{\rm GS2}) - C_{\rm GIZO}(V_{\rm GS1})}{\pi r^2 \times T_{\rm GIZO}} \\ &= \frac{q\Delta n}{\Delta V_{\rm GS}} \\ &= \frac{q \int_{(E_F-E_i)(V_{\rm GS1})}^{(E_F-E_i)(V_{\rm GS2})} g(E)dE}{\Delta V_{\rm GS}} \; [\rm F \cdot cm^{-3}] \end{aligned} \qquad (5)$$

$g(E)$ is extracted by using

$$g(E) = \frac{\Delta C'_{\rm GIZO}}{q^2}, \quad (E_F - E_i)(V_{\rm GS1}) < E < (E_F - E_i)(V_{\rm GS2}) \; [\rm eV^{-1} \cdot cm^{-3}] \qquad (6)$$

where $r(= 25\ \mu\rm m)$, $E_F(V_{\rm GS})$, and $\Delta V_{\rm GS}(= 303\ \rm mV)$ are the radius of the optical fiber used in the photon-illumination, the quasi-Fermi level as a function of $V_{\rm GS}$, and the resolution of swept $V_{\rm GS}$ in the C–V measurement, respectively. As seen in (4)–(6), we note that the photoresponsive energy range of $g(E)$ is modulated by both the surface potential (ϕ_s) through $V_{\rm GS}$ and $E_{\rm ph}$. The $g(E)$ is assumed to uniformly be distributed along the a-GIZO depth direction, and this is valid as far as the energy band bending is not so steep over the region. In terms of matching the energy level, two transition points in the C–V curve are assumed to correspond to E_i (midgap) and E_C, respectively, as shown in the inset of Fig. 2.

In order to confirm a comprehensible charge pumping by the optical source, $P_{\rm opt}$-dependent C–V responses are investigated. As shown in Fig. 3(a), the optical response of the C–V characteristics saturates at the optical excitation with $P_{\rm opt} \sim$ 41 mW. This reflects that the total trapped charges in the corresponding energy levels are sufficiently excited by photons over $P_{\rm opt} > 41$ mW. Fig. 3(b) shows the extracted $g(E)$ as a superposition of the exponential tail states and the Gaussian deep states, as is the case in a-Si:H TFT's [8]. In the C–V curve under $P_{\rm opt} = 50$ mW for $V_{\rm GS} = -5$ V and 1.4 V (the value of 1.4 V was consistent with the linearly extrapolated threshold voltage V_T) are matched to E_i (midgap) and E_C, respectively, assuming that ϕ_s is a function proportional to $V_{\rm GS}$. Consequently extracted $g(E)$ is modeled as

$$g(E) = N_{\rm TA} \times \exp\left(\frac{E - E_C}{kT_{\rm TA}}\right) + N_{\rm DA}\exp\left[-\left(\frac{E_O - E}{kT_{\rm DA}}\right)^2\right]$$

with extracted model parameters as $N_{\rm TA} = 2 \times 10^{18}\ \rm eV^{-1} \cdot cm^{-3}$, $N_{\rm DA} = 4 \times 10^{15}\ \rm eV^{-1} \cdot cm^{-3}$, $kT_{\rm TA} = 0.085$ eV, $kT_{\rm DA} = 0.5$ eV, and $E_O = 1$ eV. In Fig. 4, measured output and transfer characteristics of a-GIZO TFTs are compared with the model obtained from a TCAD simulation [9] incorporating the extracted $g(E)$. The model reproduces measured characteristics very well for a wide range of $V_{\rm GS}$ and $V_{\rm DS}$ by considering the consistent process-controlled parameters including the effective DOS in the conduction and valence bands $N_C = N_V = 10^{19}\ \rm cm^{-3}$, $n = 3.98 \times 10^{16}\ \rm cm^{-3}$, ϕ_B (Schottky barrier height) = 2.7 eV, and $\mu_{\rm FE}$ (field-effect mobility) = 10 $\rm cm^2/V \cdot s$ (note that a single parameter set, not fitting parameters, is used with various $V_{\rm GS}/V_{\rm DS}$).

IV. Conclusion

A subbandgap optical charge pumping-based extraction technique combining the C–V characteristics for the DOS $g(E)$ in a-GIZO TFTs is proposed and verified by comparing the measured characteristics with TCAD simulation results incorporating the extracted $g(E)$. Although an improvement of the proposed model is necessary for better description of nonuniform potential profile along the depth direction, nonlinear relationship between $V_{\rm GS}$ and ϕ_s, and a possible asymmetric donorlike states, our results show that the proposed model is very useful for the device design and modeling of a-GIZO TFTs as a representative of multicomponent amorphous oxide semiconductor TFTs.

ACKNOWLEDGMENT

The authors would like to thank I.-C. Choi, S.-W. Kong, W.-S. Lee, and M.-G. Hwang of SILVACO KOREA for supporting TCAD simulations.

REFERENCES

[1] Y. Orikasa, N. Hayashi, and S. Muranaka, "Effects of oxygen gas pressure on structural, electrical, and thermoelectric properties of $(ZnO)_3In_2O_3$ thin films deposited by rf magnetron sputtering," *J. Appl. Phys.*, vol. 103, no. 11, pp. 113 703-1–113 703-7, Jun. 2008.

[2] K. Nomura, H. Ohta, A. Takagi, T. Kamiya, M. Hirano, and H. Hosono, "Room-temperature fabrication of transparent flexible thin-film transistors using amorphous oxide semiconductors," *Nature*, vol. 432, no. 7016, pp. 488–492, Nov. 2004.

[3] E. Fortunato, A. Pimentel, A. Gonçalves, A. Marques, and R. Martins, "High mobility amorphous/nanocrystalline indium zinc oxide deposited at room temperature," *Thin Solid Films*, vol. 502, no. 1/2, pp. 104–107, Apr. 2006.

[4] R. Martins, P. Barquinha, I. Ferreira, L. Pereira, G. Gonçalves, and E. Fortunato, "Role of order and disorder on the electronic performances of oxide semiconductor thin film transistors," *J. Appl. Phys.*, vol. 101, no. 4, pp. 044 505-1–044 505-7, Feb. 2007.

[5] A. Suresh, P. Wellenius, and J. F. Muth, "High performance transparent thin film transistors based on indium gallium zinc oxide as the channel material," in *IEDM Tech. Dig.*, 2007, pp. 587–590.

[6] H.-H. Hsieh, T. Kamiya, K. Nomura, H. Hosono, and C.-C. Wu, "Modeling of amorphous $InGaZnO_4$ thin film transistors and their subgap density of states," *Appl. Phys. Lett.*, vol. 92, no. 13, pp. 133 503-1–133 503-3, Apr. 2008.

[7] M. Kimura, T. Nakanishi, K. Nomura, T. Kamiya, and H. Hosono, "Trap densities in amorphous-$InGaZnO_4$ thin-film transistors," *Appl. Phys. Lett.*, vol. 92, no. 13, pp. 133 512-1–133 512-3, Apr. 2008.

[8] C. R. Kagan and P. Andry, *Thin-Film Transistors*. New York: CRC Press, 2003, pp. 77–78.

[9] *Atlas Users Manual*, Silvaco Int., Santa Clara, CA, 2005. [Online]. Available: http://www.silvaco.com